The effect of the molecular structure of hydroxypropyl methylcellulose on the states of water, wettability, and swelling properties of cryogels prepared with and without calcium peroxide

Camila Gruber Chiaregato[1], Oigres Daniel Bernardinelli[2], Amin Shavandi[3], Edvaldo Sabadini[4] and Denise Freitas Siqueira Petri[1]

1. Department of Fundamental Chemistry, Institute of Chemistry, University of São Paulo, 05508-000, São Paulo, Brazil
2. Department of Physics, Federal University of São Carlos, 13565-905, São Carlos, Brazil
3. BioMatter Unit, École Polytechnique de Bruxelles, Université Libre de Bruxelles (ULB), 1050 Brussels, Belgium
4. Department of Physical Chemistry, Institute of Chemistry, State University of Campinas, 6154,13083-970, Campinas, Brazil

Abstract

Hydroxypropyl methylcellulose (HPMC) belongs to the cellulose ether family that has both hydrophobic methyl groups (DS) and hydrophilic hydroxypropyl groups (MS) on its chain. Herein, the interactions between water molecules and cryogels prepared with HPMC in the presence and absence of a linear nonionic surfactant containing a dodecyl chain and a PEG chain, as well as CaO_2 microparticles, which react with water producing O_2, were systematically investigated by sorption experiments and Time-Domain Nuclear Magnetic Resonance (TDNMR). Regardless of the DS and MS, most water molecules presented transverse relaxation time t2 typical of intermediate water and a small population of more tightly bound water. HPMC cryogels with the highest DS of 1.9 presented the slowest swelling rate of 0.519 ±0.053 $g_{water}/(g.s)$ and the highest contact angle values 85.2500º ± 0.0039º, providing the best conditions for a slow reaction between CaO_2 and water. When the surfactant is present, it may create hydrophobic interactions that allow the polar head of the surfactant to be exposed to the medium, resulting in a higher swelling rate and lower contact angle values. The HPMC with the highest MS presented the fastest swelling rate and the lowest contact angle. These findings are relevant for the formulations and reactions, where tuning the swelling kinetics is crucial for the final application.

Keywords: hydroxypropyl methylcellulose, transverse relaxation time, swelling rate, contact angle, CaO_2

1 Introduction

Understanding the interactions between polysaccharides and water allows the preparations of materials with tunable properties. For instance, the degree of swelling and dissolution of polysaccharides in food formulations affect the texture and consistency of the final products (Dedhia et al., 2022; Y. Wei et al., 2021). Polysaccharides are commonly used as protective materials in drug formulations due to their biocompatibility (Barclay et al., 2019; Kurczewska, 2022). The sustained release of the drug depends on the swelling and erosion rate of the polysaccharide layer, which is controlled by the polysaccharide molecular structure (Khalid et al., 2021). In the field of construction and building materials such as gypsum paste (Liu et al., 2021) or cement (Schmidt et al., 2017) the addition of polysaccharides can tune their rheological properties.

Hydroxypropyl methylcellulose (HPMC) or hypromellose belongs to a family of cellulose mixed ethers resulting from the substitution of hydroxyl groups by methyl and hydroxypropyl groups. The degree of substitution (DS) and the molar substitution (MS) refer to the number of moles of methyl group and of hydroxypropyl groups per mole of repeated unit, respectively. Hydroxypropyl groups can undergo chain reactions, increasing the MS value. HPMC samples with high DS values tend to be more hydrophobic, whereas samples with high MS values tend to be more hydrophilic (Thielking & Schmidt, 2006). The solubility of HPMC in water tends to improve when the system is cooled, as lower temperatures decrease the entropy of water, which promotes the hydration of HPMC chains (Tundisi et al., 2021). When the system is heated, the entropy of water molecules increases, leading to dehydration of the HPMC chains and an increase in hydrophobic interactions between the methyl groups. Some trends were found based on the rheological behavior and scattering properties of aqueous solutions of HPMC. When the concentration of HPMC in an aqueous solution exceeds the critical overlap concentration, which is related to the entanglement of polymer coils, the solution undergoes phase separation upon heating up to ~ 50 ^{o}C (Lodge et al., 2018). This phase separation temperature is not affected by the heating rate (thermodynamic phase transition), but it does depend on the HPMC concentration, DS, MS, and molecular weight (Lodge et al., 2018). The increase in the DS values tends to decrease the temperature at which such phase transitions take place (Perez-Robles et al., 2022).

The structure of water molecules in polysaccharide hydrogels depends on the chemical structure of the polysaccharide. In general, water molecules can be found in three different states: (i) non-freezing bound water molecules, which are not freezable due to the strong interaction with the polymer chains, (ii) freezing bound water or intermediate water, which freezes below 0 ^{o}C due to the less strong interactions between water and polymer chains, and

(iii) free water (Hatakeyama & Hatakeyama, 2017). Experimentally, these states of water can be detected by calorimetry and Time-Domain Nuclear Magnetic Resonance (TDNMR). TDNMR is a powerful tool to determine the states of water in hydrogels because free water molecules have t2 relaxation time of typically greater than thousands of ms (Toledo et al., 2020), whereas non-freezing bound water molecules have t2 in the order of units of ms (Wang et al., 2020; S. Wei et al., 2018). t2 values of typically hundreds of ms are assigned to freezing bound water or to water molecules that form “water pools" in hydrogels (da Silva et al., 2022). Trp modified HPMC cryogels presented populations of water molecules with t2 relaxation time in the range of 200 ms to 400 ms, indicating that the modification favored the state of freezing bound water. The adsorptive capacity of HPMC-Trp cryogels towards methylene blue and rhodamine B increased with the increase of the fraction of freezing bound water molecules, which was caused by the progressive increase of Trp content (Toledo et al., 2020). Vanillin modified chitosan hydrogels presented swelling degree and populations of freezing bound water molecules that decreased with the increase of vanillin content due to the hydrophobicity (da Silva et al., 2022).

HPMC cryogels can be formed upon freeze-drying hydrogel precursors. In the presence of citric acid, the heating of dry cryogels at 165 ^{o}C for 5 min promotes the esterification reaction between the HPMC hydroxyl groups and carboxylic acid groups (Martins et al., 2017), rendering stability in the pH range from 0 to 9, and above pH 9 the ester linkages undergo hydrolysis. Citric acid can be used as crosslinker between two HPMC chains and as a linker between HPMC chains and β-cyclodextrin (de Souza & Petri, 2018), amino acids (Toledo et al., 2020), or sugarcane bagasse microparticles (Dias et al., 2022). When crosslinked and tryptophan (Trp) modified HPMC cryogels are immersed in water, they can uptake up to 47 grams of water per gram of cryogel (Toledo et al., 2020).

The interactions between polysaccharides and water might affect certain reactions. For instance, calcium peroxide (CaO_2) reacts with water producing oxygen (O_2) (eq. 1) and/or H_2O_2 (eq. 2), which is decomposed to O_2 (eq. 3). For this reason, CaO_2 is often used for wastewater treatment, restoration of eutrophic aquatic systems and soil remediation (Lu et al., 2017). However, the direct application of CaO_2 to ground water generates $Ca(OH)_2$, increasing the pH of the surrounding medium, and affecting indigenous microorganisms (Kao et al., 2003). Although poly(vinyl pyrrolidone), poly(ethylene glycol) and poly(vinyl alcohol) have been applied as protective layers of CaO_2 nanoparticles (Ali et al., 2020), there is scarce information about the use of polysaccharides to retard the reaction between CaO_2 and water (Lee et al., 2014).

$CaO_2 + H2O \rightarrow Ca(OH)_2 + ½\ O2$ (1)

$CaO_2 + 2H_2O \rightarrow Ca(OH)_2 + H_2O_2$ (2)

$H_2O_2 \rightarrow H_2O + ½\ O_2$ (3)

In this work, cryogels were prepared with three HPMC samples of similar molecular weight, but different DS and MS. These cryogels were then modified by incorporating a nonionic surfactant called Alkonat-L230® which contains a dodecyl chain and a PEG chain and/or CaO_2 microparticles. The choice of Alkonat-L230® was based on its wetting properties and the lack of previous studies using this kind of surfactant. The hypothesis is that a preferential orientation of surfactant molecules towards the HPMC functional groups can influence the wetting properties, swelling degree and the states of water of the cryogels. Furthermore, it is hypothesized that incorporating CaO_2 microparticles into HPMC cryogels (modified or not by the surfactant) should retard the reaction between water and CaO_2, providing a more sustained release of oxygen compared to pure CaO_2. Thus, this study was developed to understand how the molecular structure of HPMC and surfactant modified HPMC affects (i) the interactions between HPMC and water, (ii) the states of water in the hydrogels and (iii) the CaO_2 decomposition to O_2.

2 Material and methods

2.1 Materials

HPMC samples kindly provided by Dow Chemical Brazil Co. with different DS and MS values, but similar molecular weights (**Table 1**), citric acid (Labsynth, Brazil, 192.12 g mol^{-1}), sodium hypophosphite (Labsynth, Brazil, 105.99 g mol^{-1}), calcium peroxide (CaO_2, Sigma-Aldrich 466271, 72.08 g mol^{-1}, ~ 75% purity, 200 mesh), Alkonat-L230® surfactant (CAS Number: 9002-92-0, 1198 g mol^{-1}, HLB 16.9, Oxiteno, Brazil), hydrochloric acid (HCl, Labsynth, 36.5% purity), Tris(hydroxymethyl)aminomethane (Tris, Sigma, 121.14 g mol^{-1}, 99.5 purity) were used as received. **Fig. 1a** and **1b** represent the chemical structure of HPMC and Alkonat-L230®, respectively. Alkonat-L230® is an uncharged surfactant obtained from the reaction between lauryl alcohol and ethylene oxide. The critical micelle concentration (cmc) was determined by tensiometry at 22 ± 1 °C as 0.084 g L^{-1} (0.07 mM), details were provided as **Fig. SM1**.

Table 1 HPMC characteristics: United States Pharmacopeia (USP) codes corresponding to the DS and MS ranges. Degree of substitution (DS), molar substitution (MS), weight average molecular weight (M_w), and viscosity average molecular weight (M_v)

HPMC type	USP code	Code	DS*	MS*	Molecular weight (g mol^{-1})

K4M	2208	HPMC-K	1.5	0.25	[(a)] M_w 2.1 x 10^5
J12MS	1828	HPMC-J	1.5	0.75	[(b)] M_v 3.5 x 10^5
E4M	2910	HPMC-E	1.9	0.25	[(a)] M_w 2.5 x 10^5

*Data provided by producer, (a) determined by gel permeation chromatography (Marani et al., 2015), (b) determined by capillary viscometry (Dezotti et al., 2021).

2.2 Preparation of HPMC/Alkonat/CaO_2 and HPMC/CaO_2 cryogels

Solutions of HPMC at 3.0 wt% containing 0.3 wt% of citric acid (crosslinker) and 0.15 wt% of sodium hypophosphite (catalyst) were prepared with MilliQ® water under magnetic stirring. For the preparation of HPMC solutions with Alkonat-L230®, Alkonat-L230® was added to the HPMC solution so that the final concentration was 0.168 g L-1 (2 x cmc). For the incorporation of CaO2 microparticles into the HPMC solutions, 50.0 mg of CaO2 was added to 1.6 g of HPMC solution. Then, the precursors were put into polypropylene tubes of 2 mL, frozen at −24 °C during 24 h (standard freezer), and then freeze dried under vacuum (0.2 bar) during 10-12 h. After that, the cryogels were oven heated to 165 °C for 5 min to promote the esterification reaction between citric acid and HPMC hydroxyl groups. The resulting cryogels were coded as shown in Fig. 1c.

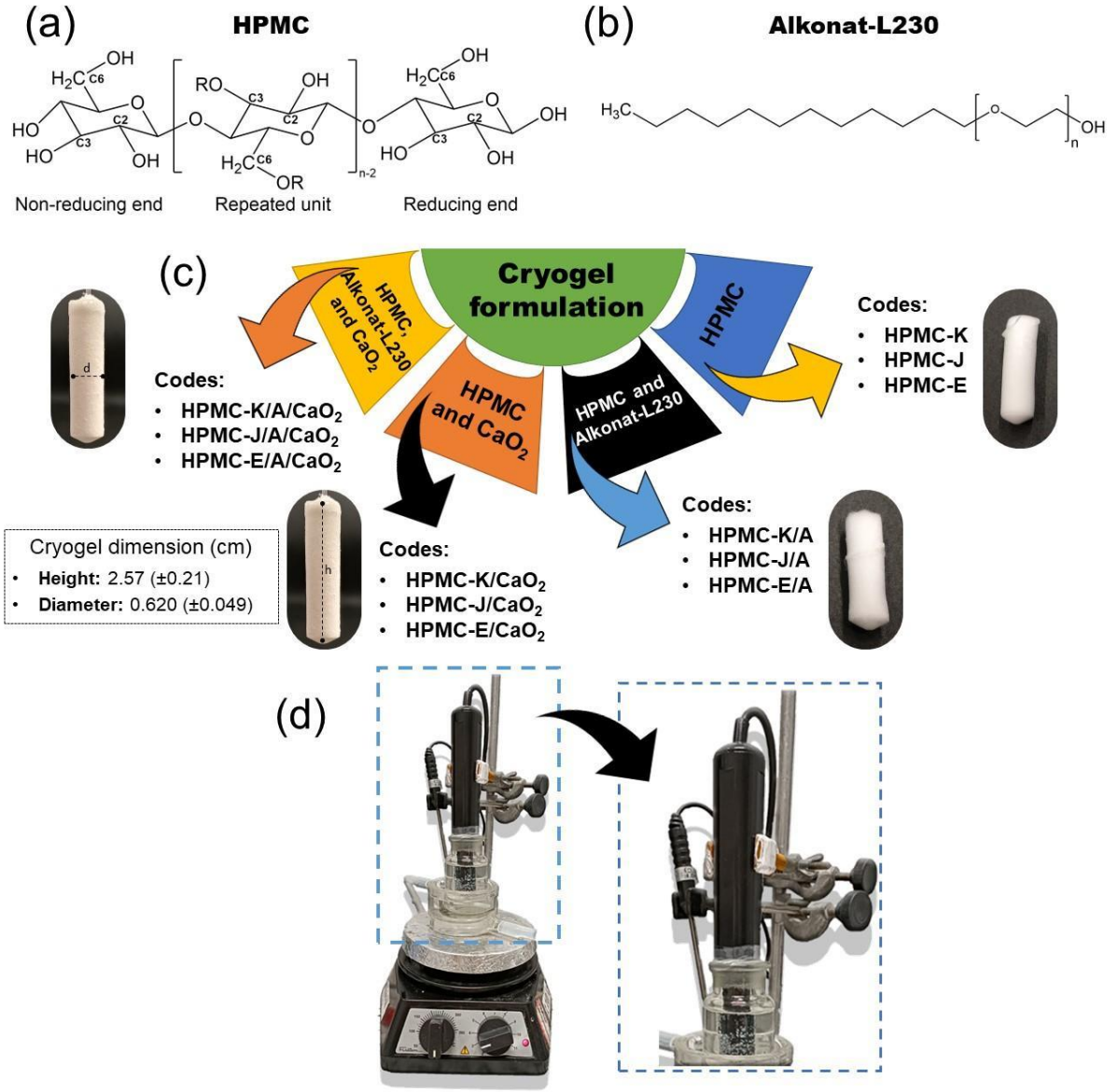

Figure 1 Schematic representation of chemical structures of (a) HPMC, where R= −H, $-CH_3$, or $-CH_2-CHOH-CH_3$; (b) Alkonat-L230®, n = 23 and dodecyl chain, coded as A. (c) Codes used for the different formulations of HPMC based cryogels and the corresponding photographs; (d) Experimental setup used for the determination of O_2 released in the aqueous medium as a function of time.

2.3 Kinetics of O_2 release

The kinetics of the reaction of CaO_2 and water was evaluated by measuring the release of O_2 (equations 1 and 3) in the aqueous medium as a function of time, using a selective O_2 sensor (Lutron WA-2015), which registered periodically the concentration of O_2 dissolved in the medium. For all the experiments, a glass vial of 60 mL was filled with 50 mL of MilliQ® water, which was previously purged with N_2 to reduce the concentration of O_2 naturally dissolved in the medium. The temperature was controlled by a thermostat (Thermo Scientific, Accel 250), and the system was kept under mild magnetic stirring during 4 h or 24 h. The

system (**Fig. 1d**) was sealed with Parafilm®. Considering that the reaction vial was practically completely filled, all O_2 produced is expected to be in the aqueous phase.

Initially, the effect of temperature, ethanol/water mixture and pH on the kinetics of the reaction between pure CaO_2 and water was evaluated by varying (i) temperature (20 °C, 25 °C, 30 °C); (ii) water concentration (water, ethanol/water 50% v/v), and (iii) pH (5.5 MilliQ® water and Tris-HCl buffer at 7.5). For all experiments, the CaO_2 concentration was set at 1 mg mL^{-1}. The results of these experiments allowed choosing the best conditions for the kinetics study using the CaO_2 incorporated in the cryogels.

2.4 Characterization

After the crosslinking reaction, the cryogels were weighed (m_{pol}), and washed (except for samples with CaO_2) with deionizer water to remove the unreacted molecules until the water reached the conductivity of ~ 5.5 µS cm^{-1}. Noteworthy, after crosslinking, the cryogels containing CaO_2 microparticles were not rinsed to avoid loss of CaO_2 by the reaction with water. Then, the cryogels were swollen with MilliQ® water, freeze-dried for the second time, weighed (m_{dried}), and used in further analyses. The gel content was calculated according to:

$$Gel(\%) = \frac{m_{dried}}{m_{pol}} \times 100 \quad (4)$$

The swelling kinetics was determined using the sorption kinetics mode of a Krüss K100 precision tensiometer (± 0.00001 g, Krüss, Hamburg Germany), at 22 ± 1 ºC. The sample was fixed at the mass sensor (**Fig. SM2**), the vessel containing MilliQ® water approached the sample automatically. Upon touching the sample, the water was sorbed by the sample and its mass was registered as a function of time. The swelling rate (SR) was determined by the initial slope of the dependence of the mass of sorbed MilliQ® water on the time. The swelling degree (SD) was calculated by dividing the mass of sorbed MilliQ® water under equilibrium conditions (m_{water}) by m_{dried}:

$$SD = \frac{m_{water}}{m_{dried}} \quad (5)$$

The contact angle of water on the cryogels was determined indirectly by the Washburn method using a K100 Krüss (Germany) tensiometer, at 22 ± 1 ºC, as shown in **Fig. SM2**. The increase of mass absorbed by the sample due to capillary forces was recorded as a function of time. First, the capillary constant (C_w) was calculated using the Washburn equation (Eq. 6), and n-hexane as liquid (contact angle θ = 0°).

$$cos\theta = \frac{m^2\eta}{t\rho^2\sigma C_w} \quad (6)$$

Where, θ (°) is the contact angle of the liquid on the solid, m (g) is the mass of liquid absorbed through capillarity, η (Pa s) is the viscosity of the liquid, t (s) is the time, ρ (g cm^{-3}) is the density of the liquid, and σ (N m^{-1}) is the surface tension of the liquid. After determining the C_w, the

sorption experiments were performed for MilliQ® water in order to find out the θ values for water on the HPMC cryogels.

The apparent density was calculated by measuring the cryogel dimensions with a pachymeter and weighting them in an analytical balance in triplicate. The apparent porosity (P_{ap}) of cryogels was calculated by

$$P_{ap} = (1 - \frac{\sigma_{ap}}{\sigma_{cell}}) \times 100 \quad (7)$$

Where, ρ_{ap} is the apparent density of cryogels and ρ_{cell} is the density of HPMC (1.3 g cm^{-3}).

FTIR analysis was done in the attenuated total reflectance mode (ATR-FTIR, Perkin Elmer Frontier), using a ZnSe crystal, resolution of 4 cm^{-1}, in the range of 600 cm^{-1} to 4000 cm^{-1}, and accumulation of 64 scans. The morphology of HPMC based cryogels was evaluated by scanning electron microscopy (SEM), using Jeol Neoscope JSM-7401F microscope, operating at 10 kV and high vacuum; all samples were previously coated with a 5 nm layer of gold.

Transverse water proton relaxation time (t2) measurements were carried out on a Bruker Minispec MQ20 (20 MHz) at 33°C using Carr-Purcell-Meiboom-Grill (CPMG) pulse sequence requiring 30000 echoes with echo time of 0.16 ms, adopting similar data approach as the reference. SKL Neo MultiExp program was used for inverse Laplace transform and Log-Normal distribution integration was aided by a user-guided program called Peakfit 4.00 (Jandel scientific software) (Toledo et al., 2020). The dried cryogels were swollen in deionized water in the weight-to-weight (w/w) ratio (between 10-30%) inside the NMR probe during TDNMR acquisition that lasted a total of 20 min.

2.5 Statistics

Statistical analysis was done using the Origin Lab software (version 2022b) with ANOVA and Tukey Test. Values of $p < 0.05$ indicated a statistically significant difference. The standard deviations were represented with two significant digits (Harris, 2019).

3 Results and discussion

3.1 Effect of DS, MS and surfactant on the physical properties of HPMC cryogels and on their interaction with water

The effects of DS, MS and the addition of a nonionic surfactant on the physical properties of HPMC cryogels and on their interaction with water were systematically investigated.

Table 2 shows the mean values of gel content (Gel%), swelling degree (SD), swelling rate (SR), and contact angle values determined for HPMC-E, HPMC-J, and HPMC-K indicated

that the sample with the largest MS value of 0.75 of HPMC-J favored the crosslinking with citric acid, increasing the Gel%. Although the SD values determined for HPMC-E, HPMC-J and HPMC-K were statistically similar, the swelling rate (SR) values were not (**Table 2** and **Fig. 2**). The SR values determined for HPMC-E, HPMC-J and HPMC-K amounted to 0.519 ± 0.053 g_{water}/(g.s), 7.29 ± 0.92 g_{water}/(g.s) and 1.54 ± 0.67 g_{water}/(g.s), respectively. The slowest water sorption was observed for HPMC-E, which has the highest DS, whereas the fastest water sorption was observed for HPMC-J, which has the highest MS. This trend was also observed for the contact angle values. The highest DS value of 1.9 rendered HPMC-E the highest contact angle value (85.2500º ± 0.0039º), whereas the lowest DS value of 1.5 led to contact angle values of 72.56º ± 0.94º and 73.5º ± 2.8º for HPMC-K and HPMC-J, respectively.

Table 2. Mean values of apparent density (ρ_{ap}), apparent porosity (P_{ap}), gel content (Gel%), swelling degree (SD), swelling rate (SR), and contact angle determined for the HPMC-E, HPMC-E/A, HPMC-J, HPMC-J/A, HPMC-K, and HPMC-K/A cryogels.

Sample	ρ_{ap} (g cm^{-3})	P_{ap} (%)	Gel%	SD (g_{water}/g)	SR (g_{water}/(g.s))	Contact angle (°)
HPMC-K	0.0477 (±0.0067)	96.33 (±0.52)	88.6 (± 7.6)	33.2 (±1.4)	1.54 (±0.67)	72.56 (± 0.94)
HPMC-J	0.0640 (±0.0015)	95.08 (±0.11)	93.6 (± 1.2)	35.1 (±3.1)	7.29 (±0.92)	73.5 (± 2.8)
HPMC-E	0.0529 (±0.0017)	95.93 (±0.13)	92.5 (± 3.3)	32.2 (±2.5)	0.519 (±0.053)	85.2500 (± 0.0039)
HPMC-K/A	0.0630 (±0.0043)	95.16 (±0.33)	92.7 (± 1.2)	35.7 (±6.3)	1.49 (±0.12)	68.5 (± 1.5)
HPMC-J/A	0.0678 (±0.0059)	94.79 (±0.45)	90.38 (± 0.37)	32.3 (±3.1)	2.46 (±0.92)	73.5 (± 3.0)
HPMC-E/A	0.0605 (±0.0054)	94.95 (±0.41)	93.1 (± 2.3)	31.7 (±1.5)	0.720 (±0.082)	80.55 (± 0.84)

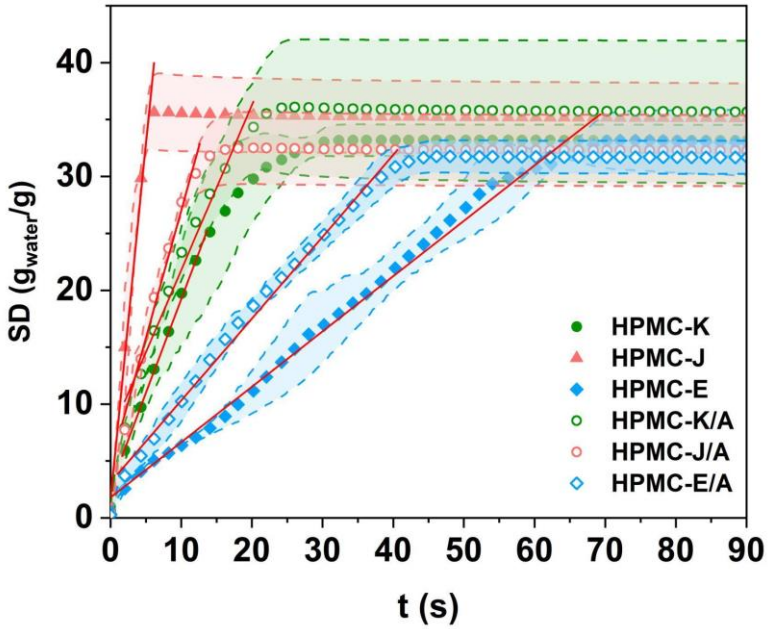

Figure 2. Mean values of swelling degree (SD) as a function of time determined for HPMC cryogels in MilliQ® water, at 22 ± 1 °C. The red lines correspond to the linear fits. The dotted lines represent the minimum and maximum values of SD determined for each system.

Regardless of the type of HPMC, the addition of Alkonat-L230® (surfactant) did not affect the Gel% and SD values, which amounted to ~ 90-93%, and 32-35 g_{water} g^{-1}, respectively (**Table 2**). Giang and co-workers (Giang et al., 2022) observed that the addition of PEG (1 wt%) to HPMC-E and citric acid (5 wt%) led to Gel% of only ~ 50%; such a low Gel% was attributed to the degradation of PEG during the thermal esterification process. However, it was not the case for the cryogels containing Alkonat-L230® because the cryogels were stable (no change of color) after heating at 165 ^{o}C to promote the esterification with citric acid and the Gel% valeus did not decrease. On the other hand, the SR values determined for HPMC-E/A (0.720 ± 0.082 g_{water}/(g.s)) were slightly larger than those for HPMC-E (0.519 ± 0.053 g_{water}/(g.s)), indicating somehow the polar head of the surfactant adsorbed on the cell walls made the environment more hydrophilic. One should notice that for the characterization, the cryogels were rinsed to remove loose HPMC chains and unreacted molecules, and freeze-dried again. Thus, the remaining Alkonat-L230® molecules are probably bound to the cryogels as monomers. This interpretation was reinforced by the decrease in the contact angle values from (85.2500^{o} ± 0.0039^{o}) to (80.55^{o} ± 0.84^{o}). Conversely, in the case of HPMC-J/A (high MS), the SR values decreased significantly, from 7.29 ± 0.92 g_{water}/(g.s) to 2.46 ± 0.92 g_{water}/(g.s). It might be due to the interactions of the Alkonat-L230® polar head to the hydroxypropyl groups (MS 1.9), exposing the hydrophobic tails, although no change was observed in the contact angle values. Tablets of HPMC K100M prepared with sodium dodecyl sulfate (SDS) presented smaller swelling degree and increased erosion than their pure counterparts due to possible

attractive hydrophobic interaction between HPMC K100M and SDS dodecyl chains (Zeng et al., 2009). The SR and the contact angle values for HPMC-K/A were statistically similar to those determined for HPMC-K, possibly due to the low MS and DS values.

There is scarce information about the interactions between HPMC and linear nonionic surfactants with structures similar to that of Alkonat-L230®. However, the interactions between Pluronic® F-127, a surfactant composed of PEO-PPO-PEO blocks, and HPMC were estimated using calculations based on the Hartree-Fock method; the interactions between HPMC-K and the hydrophilic PEO blocks were more favorable (−30 kcal/mol) than those between HPMC and the hydrophobic PPO blocks (− 22 kcal/mol) (da Silva et al., 2021). This trend corroborates with the most pronounced effects of Alkonat-L230® on the SR and contact angle values determined for HPMC-J/A (highest MS).

Fig. SM3 shows the FTIR-ATR spectra obtained for all HPMC based cryogels. HPMC cryogels containing Alkonat-L230® showed no shift in the characteristic peaks and absence of new peaks, in comparison to the spectra of each pure HPMC cryogel and pure Alkonat-L230® because they have similar functional groups (Parhi, 2016). All cryogels presented the typical HPMC s (assignments available in the **Fig. SM3**), and the esterification between citric acid and HPMC chains was identified by the band at 1732 cm^{-1}, which was assigned to C=O stretching of the ester group (Toledo et al., 2020).

Fig. 3 shows the SEM images obtained for the HPMC-K, HPMC-J, HPMC-E, HPMC-K/A, HPMC-J/A, and HPMC-E/A cryogels. All cryogels presented open isotropic macropores ranging from ~ 20 µm to 100 µm. The presence of Alkonat-L230® led to a slight increase in the ρ_{ap} values, which might be associated with the favorable interactions between HPMC and Alkonat-L230®.

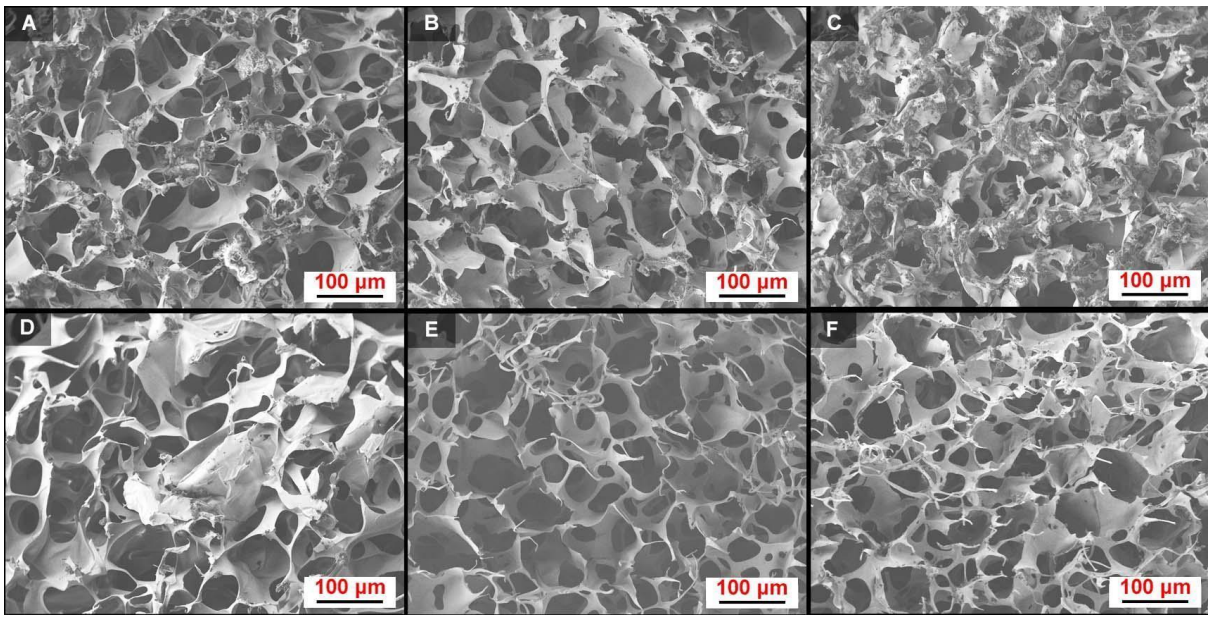

Figure 3. SEM imagens for the (A) HPMC-K, (B) HPMC-J, (C) HPMC-E, (D) HPMC-K/A, (E) HPMC-J/A, and (F) HPMC-E/A cryogels.

The transverse water proton relaxation time (t2) was used to determine the states and locations of water pools within HPMC based cryogels. **Fig. 4** shows the distribution of t2 obtained for HPMC-K, HPMC-J, HPMC-E, HPMC-K/A, HPMC-J/A and HPMC-E/A cryogels, and **Table SM4** presents the corresponding populations. All samples showed water molecules mostly (90-96%) distributed in the intermediate t2 values (100 ms - 10000 ms) and a small population (4-10%) in the t2 range of 10 ms to 100 ms. They presented similar distributions of t2 probably because they have similar heterogeneous and interconnected structures (open isotropic macropores ranging from ~ 20 µm to 100 µm), as observed in **Fig. 3**. One should notice that the measurements were performed at swelling equilibrium conditions, when these samples presented similar SD values (**Table 2**), and there was no bulk water. For comparison, the t2 distribution was measured for Avicel® microcrystalline cellulose under similar conditions. The distribution of t2 observed between 100 ms and 1000 ms was narrower than those observed for the HPMC based cryogels, and no t2 signal was detected below 100 ms. It means that the substitution of cellulose hydroxyl groups by methoxy and hydroxypropyl groups created small heterogeneous sites, where the water molecules became stiffer.

Physical hydrogels of HPMC K presented t2 of 1865 ms and 7.4 ms, corresponding to free and bound water (Baumgartner et al., 2002). Citric acid crosslinked HPMC chains, creating a tighter network and smaller pores for water than those in physically crosslinked HPMC hydrogels. Moreover, in Fig. 4 no signal was observed for t2 larger than 1000 ms because there was no excess of water (bulk water).

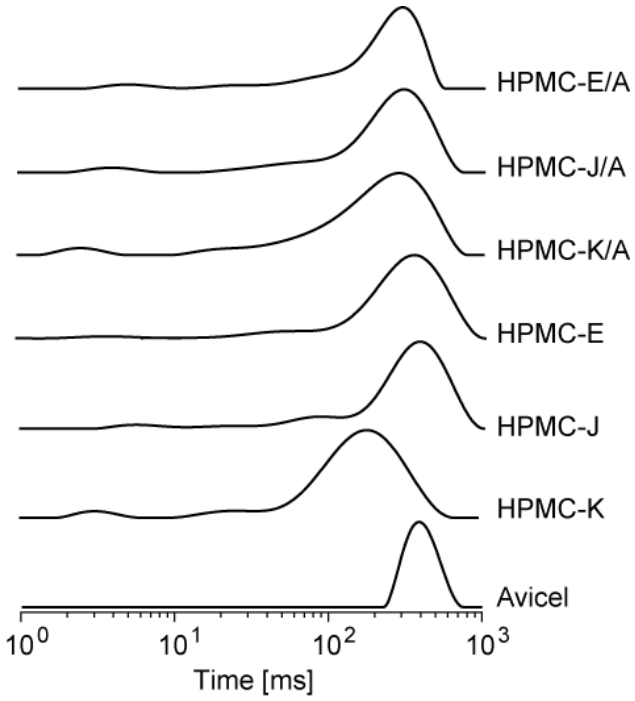

Figure 4. Transverse water proton relaxation time (t2) distribution measured by TDNMR for (a) Avicel, HPMC-K, HPMC-J, HPMC-E, HPMC-K/A, HPMC-J/A and HPMC-E/A cryogels. All cryogels were swollen in MilliQ water.

3.2 Reaction of water with CaO_2 microparticles incorporated in the HPMC cryogels

CaO_2 microparticles were incorporated in the HPMC cryogels in the absence and in the presence of Alkonat-L230®. One should notice that gel content, swelling degree, swelling rate, and contact angle were not determined for HPMC cryogels containing CaO_2 microparticles due to the reaction of CaO_2 and water. **Fig. 5** shows the SEM images obtained for the HPMC-K/CaO_2, HPMC-J/CaO_2, HPMC-E/CaO_2, HPMC-K/A/CaO_2, HPMC-J/A/CaO_2, and HPMC-E/A/CaO_2 cryogels. **Fig. SM5** shows a typical SEM image of commercial CaO_2 microparticles used in this work; it shows amorphous agglomerates of different sizes. Such agglomerates were also observed on the cell walls of all types of cryogels (**Fig. 5**), making the cell walls rougher and more heterogeneous than those observed in **Fig. 3.** The incorporation of CaO_2 microparticles in the cryogels increased approximately twofold the mean density values (**Table SM6**). The commercial CaO_2 sample is a mixture of ~ 75% CaO_2 (2.91 g cm^{-3}) and ~ 25% CaO (3.34 g cm^{-3}) and has a much higher density than HPMC (1.36 g cm^{-3}) (Doerr et al., 2018).

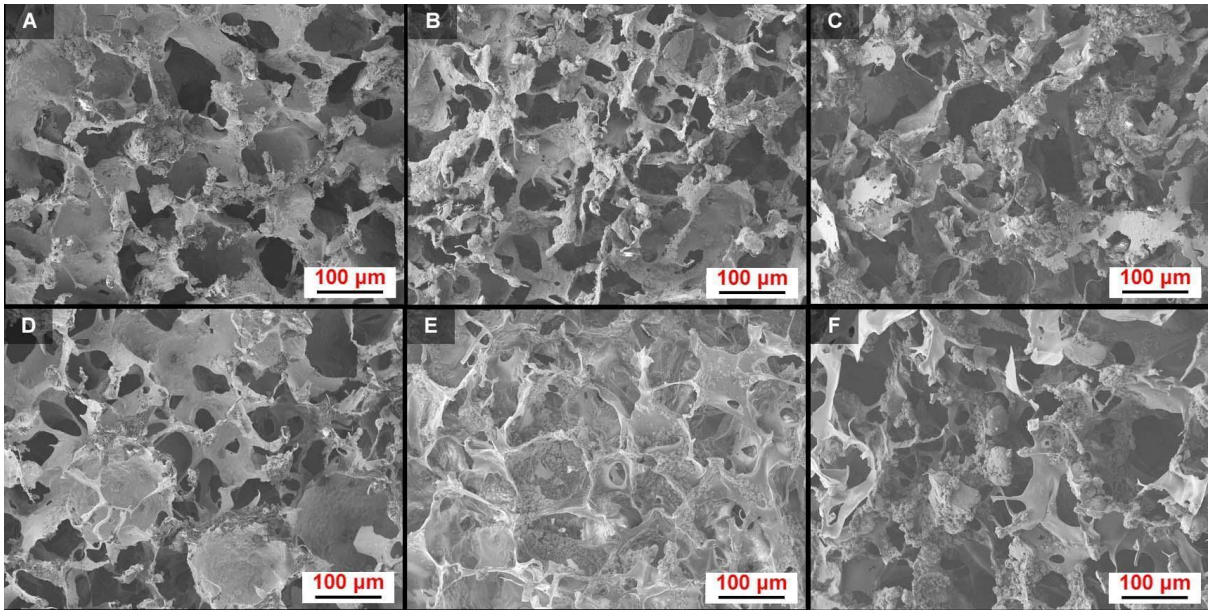

Figure 5. SEM imagens for the (A) HPMC-K/CaO_2, (B) HPMC-J/CaO_2, (C) HPMC-E/CaO_2, (D) HPMC-K/A//CaO_2, (E) HPMC-J/A//CaO_2, and (F) HPMC-E/A//CaO_2 cryogels.

The reaction of CaO_2 (solid) with water (eq. 1 and 2) produces O_2 and $Ca(OH)_2$ (eq. 1) or $Ca(OH)_2$ and H_2O_2 (eq. 2), with further decomposition of H_2O_2 into H_2O and O_2 (eq. 3). In all experiments, CaO_2 was the limiting reagent, and the amount of water was large enough to remain nearly constant. **Fig. 6a and SM7** show that in the initial stage, the concentration of O_2, [O_2], in the aqueous medium increased fast and linearly as a function of time (t). Then, after approximately one hour, the amount of O_2 in the aqueous medium did not increase linearly with the time, evidencing that the reaction became slower, until a constant value was achieved. This behavior is probably due to the fact that the surface area of the CaO_2 undergoes changes during the reaction, exposing physical and chemical heterogeneities; for instance, the sample area might be covered by $Ca(OH)_2$ formed, reducing the production of O_2. A similar case of surface erosion is the heterogeneous reaction between magnesium and aqueous hydrochloric acid that produces Mg^{2+} ions and H_2 (Birk & Walters, 1993). Thus, only the slope of the initial stage was considered for the calculation of the initial rate (V_0) of the reaction, which was based on the rate of O_2 production.

Preliminary experiments were done to evaluate the effect of the temperature on the reaction of pure CaO_2 (at 1.0 mg mL^{-1}) and H_2O (MilliQ® water, pH 5.5). **Fig. SM7a** shows the increase of [O_2] in the aqueous medium as a function t at 20 °C, 25 °C, and 30 °C. Already after 5 min, the [O_2] in the aqueous medium was considerably high (burst release) and the pH increased to 11. The V_0 values (**Fig. SM7c** and **SM7e**) determined at 20 °C, 25 °C, and 30 °C were 0.0840 ±0.0021 mg mL^{-1} min^{-1}, 0.0401 ±0.0078 mg mL^{-1} min^{-1}, and 0.037 ±0.061 mg mL^{-1} min^{-1}, respectively. The [O_2] at the plateau (after 2 h) also decreased as the temperature increased. This trend is in agreement with the exothermic behavior of the dissolution of CaO_2

observed by Northup and Cassidy (Northup & Cassidy, 2008). However, Wang and co-workers observed that the temperature increase accelerated the release rate of O_2 and H_2O_2 (Wang et al., 2016). In the present work, the temperature of 20 °C was chosen to further study the reactions involving CaO_2 incorporated into the HPMC cryogels.

The reaction of pure CaO_2 (at 1.0 mg mL^{-1}) in a mixture of H_2O/ethanol (50 % v/v), at 20 °C, was monitored as a function of time (**Fig. SM7b**). The V_0 value (**Fig. SM7d** and **SM7e**) amounted to 0.0550 ±0.0021 mg mL^{-1} min^{-1}, which is ~ 65% of the V_0 value determined for the reaction in pure water (0.0840 ±0.0021 mg mL^{-1} min^{-1}), and the [O_2] at the plateau (after 2 h) also decreased significantly, evidencing the crucial role of H_2O as reactant (solvent).

The pH plays an important role in the reaction of CaO_2 with H_2O because the product $Ca(OH)_2$ is alkaline; as previously mentioned, the pH increased from 5.5 to 11 in 5 min of reaction. Northup and Cassidy (Northup & Cassidy, 2008) and Wang et al. (Wang et al., 2016) observed that the rate of CaO_2 dissolution increased markedly with decreasing pH, because the equilibrium reaction is favored in the products direction. **Fig. 6a** shows the [O_2] as a function of time, produced in a buffered medium (pH 7.5, Tris-HCl); the V_0 value was 0.141 ±0.014 mg mL^{-1} min^{-1} (**Fig. 6b**), which is larger than that determined at pH 11 (0.0840 ±0.0021 mg mL^{-1} min^{-1}). Also, it is possible to observe the burst release effect (Rastinfard et al., 2017; Steg et al., 2015), because after ~ 2 h the release of O_2 decreased.

Fig. 6a shows the [O_2] as a function of time measured for CaO_2 microparticles incorporated in the HPMC cryogels in the absence and in the presence of Alkonat-L230®, at 20 °C and pH 7.5 (Tris-HCl buffer). **Fig. 6b** shows the V_0 values determined for each system. The release of O_2 from any of the cryogels was slower than that observed for pure CaO_2, there was no burst effect and even after 4 h, the [O_2] tended to increase, indicating a sustained release behavior. The type of HPMC used to prepare the cryogels or the presence of Alkonat-L230® in the cryogels exerted no statistically significant effect on the V_0 values. Although the SR and contact angle values determined for the cryogels indicated different interaction with water, the SD values under equilibrium were similar (**Table 2**), and that might be the reason for the similar V_0 values. Nevertheless, after 4 h, the amount of O_2 released to the medium from HPMC cryogels prepared with Alkonat-L230® was slightly larger than that released from the HPMC cryogels free of surfactant, particularly for the systems HPMC-E/CaO_2 and HPMC-E/A/CaO_2. Considering that HPMC-E and HPMC-E/A presented the smallest SR and highest contact angle values (**Table 2**), this system was chosen to evaluate the amount of O_2 released over 24 h.

The trend observed in **Fig. 6a** was confirmed in the release experiment over 24 h (**Fig. 6c**), where the typical burst effect from pure CaO_2 was observed. The curve can be divided

into three regions: (i) the initial 30 min, when the highest amount of O_2 was released quickly; (ii) from 30 min to ~ 5 h, the release rate decreased and (iii) from ~ 5 h to 24 h the release rate was the slowest. The highest amount of released O_2 from CaO_2 incorporated in the HPMC-E and HPMC-E/A cryogels were observed after 4 h and 8 h, respectively, mitigating the burst effect observed for pure CaO_2. The decrease of the release rate of O_2 was more sustained from CaO_2 incorporated in the HPMC-E than that from CaO_2 incorporated in the HPMC-E/A cryogels. These findings can be correlated with the significant decrease of the contact angle values observed for HPMC-E/A in comparison to HPMC-E (**Table 2**).

Thus, it is possible to conclude that the incorporation of CaO_2 microparticles into HPMC cryogels is advantageous when the burst release should be avoided. The mechanism seems to be the same as that observed for the release of drugs. HPMC is frequently used for drug formulation due to its slow dissolution rate, which retards the dissolution and diffusion of the drug to the medium (Li et al., 2010; Talasaz et al., 2008; Zarmpi et al., 2020). Upon contact with water, HPMC chains swell, increasing the local viscosity. The swollen layer acts as a barrier for the diffusion of O_2 to the medium, retarding its release to the medium. Among the three types of HPMC chosen for this study, HPMC-E would be most adequate for the incorporation of CaO_2 microparticles due to the smallest SR and the highest contact angle values (**Table 2**).

Fig. 7 shows the t2 distribution measured for the HPMC cryogels in the absence and in the presence of Alkonat-L230®, containing CaO_2 microparticles, swollen in MilliQ® water for 20 min; the pH was 11 (initially pH 5.5). The measurements in the buffer were not done to avoid additional signals from the Tris-HCl, but the reaction products are the same as in MilliQ® water. The isotropic reorientation of water molecules in the bulk (free water) has characteristic correlation time larger than thousands of ms, which is due to the fast isotropic reorientation modulates their intermolecular 1H-1H dipolar interaction. The behavior of populations with t2 greater than thousands of ms is observed in cryogels when there is water in excess(bulk water). This was observed for HPMC-K/CaO_2, HPMC-E/CaO_2 and HPMC-K/A/CaO_2 cryogels (a fraction of free water greater than 50%) suggesting a collapse of the porous structure. On the other hand, the anisotropic reorientation of water molecules confined in cryogels, “water pools”, correspond to intermediate t2 values (tens and hundreds of ms), which depend on the size (diameter), heterogeneity and interconnection of the “water pools”. In the HPMC-K/CaO_2, HPMC-E/CaO_2 and HPMC-K/A/CaO_2 cryogels a broad distribution of t2 population was observed, evidencing diffusion of water (migration between distinct diameter pools sizes) and reinforcing structure collapse. It might be due to the fact that upon increasing the pH to 11, some ester bonds between citric acid (crosslinker) and HPMC hydroxyl groups might have been hydrolyzed. On the other hand, slow t2 (greater than thousands of ms) signals were not observed for the HPMC-J/CaO_2 HPMC-J/A/CaO_2 and HPMC-E/A/CaO_2 cryogels, indicating

that the cohesive structure was kept. The presence of Alkonat-L230® avoided the diffusion of water from more confined “pools” to the bulk state (t2 > 1000 ms) only in the case of HPMC-E. Thus, the preferential orientation of Alkonat-L230® molecules on the HPMC-E increased the hydrophilicity (decreased the contact angle) and stabilized the network structure.

The appearance of t2 signals in the 1 ms to 100 ms range for all cryogels might be related to the increase in the concentration of H_2O_2 in the solution (eq. 2) (Buljubasich et al., 2010). As reported in the literature (Buljubasich et al., 2010), in aqueous solutions of H_2O_2 the exchange between protons is very complex, making a direct correlation of t2 with H_2O_2 concentration very difficult, but it surpasses any other effect such as the presence of a metal-containing porous medium or production of oxygen bubbles. The presence of H_2O_2 is expected because it is the product of eq. 2, and its decomposition is slow (Marzzacco, 2001; Pędziwiatr et al., 2018).

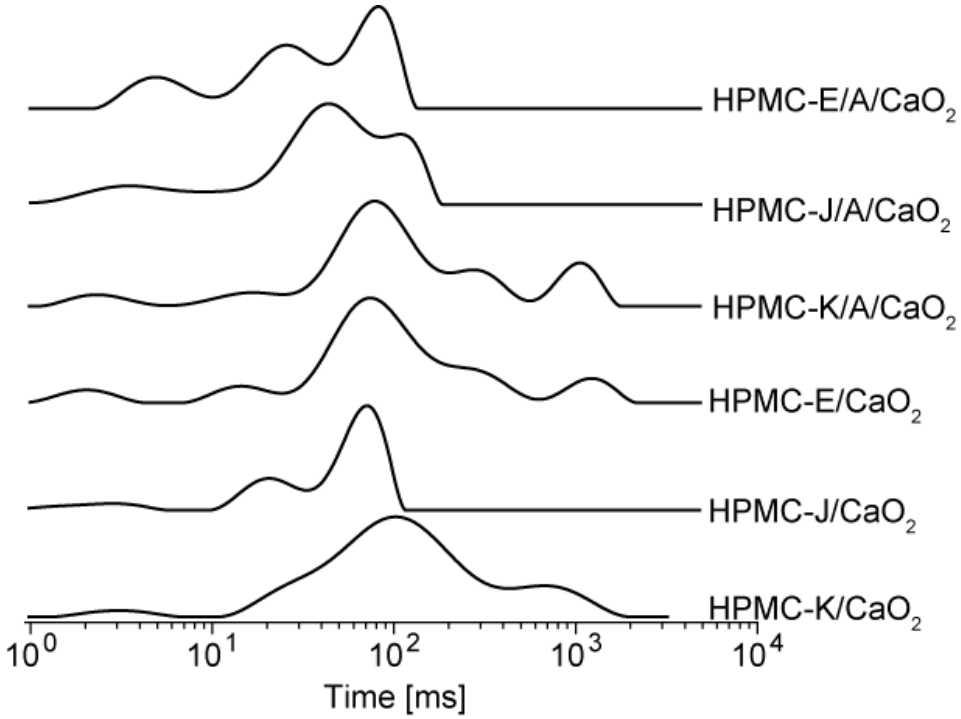

Figure 7. Transverse water proton relaxation time (t2) distribution measured by TDNMR for HPMC-K/CaO_2 HPMC-J/CaO_2 HPMC-E/CaO_2, HPMC-K/A/CaO_2, HPMC-J/A/CaO_2, HPMC-E/A/CaO_2 cryogels. All cryogels were swollen in MilliQ water.

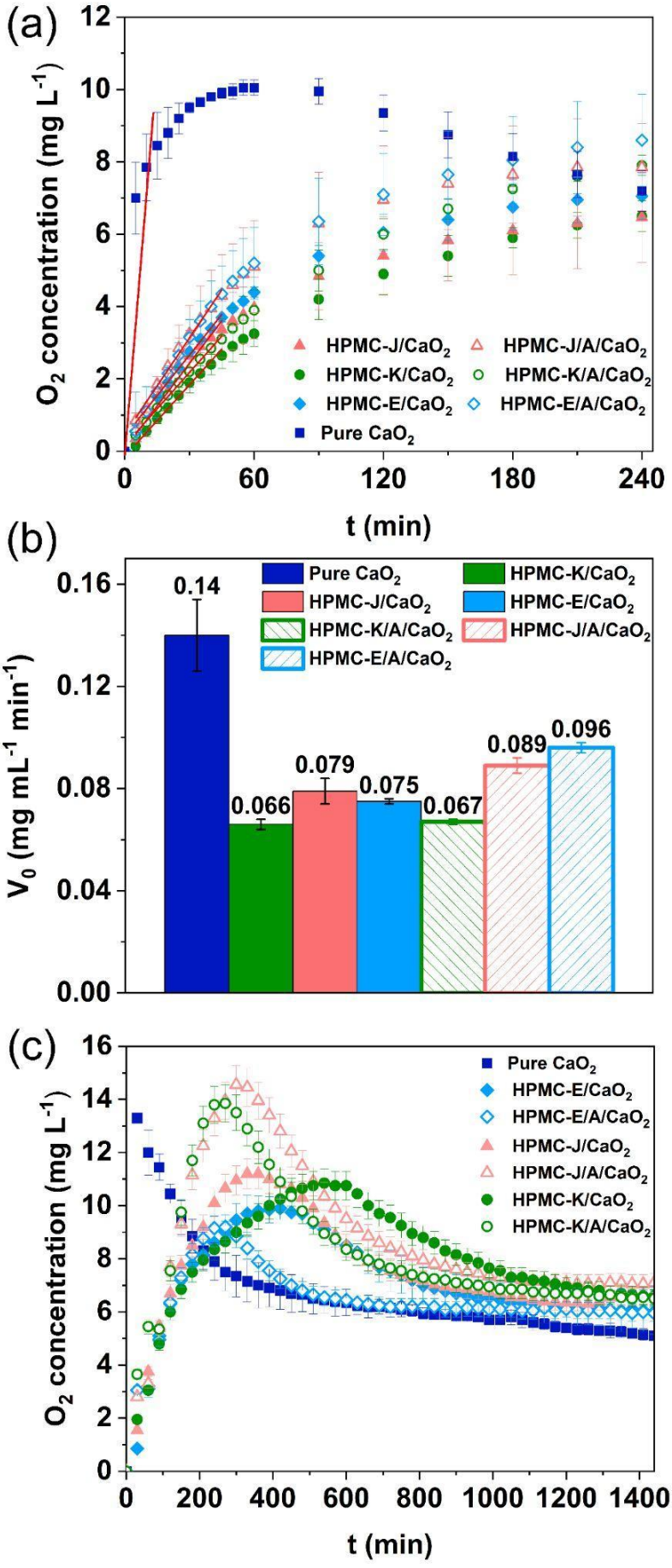
(a)
O2 concentration (mg L-1)
t (min)
HPMC-J/CaO2
HPMC-J/A/CaO2
HPMC-K/CaO2
HPMC-K/A/CaO2
HPMC-E/CaO2
HPMC-E/A/CaO2
Pure CaO2
(b)
V0 (mg mL-1 min-1)
0.14
0.066
0.079
0.075
0.067
0.089
0.096
(c)
O2 concentration (mg L-1)
t (min)

Figure 6. Kinetics of O_2 release at 20.0 ± 0.1 °C and pH 7.5 (Tris-HCl buffer) from (a) HPMC cryogels and pure CaO_2, (b) V_0 calculated from the linear fittings in the initial stage. (c) Release of O_2 from pure CaO_2, CaO_2 incorporated in HPMC-E and HPMC-E/A cryogels over 24 h, at 20.0 ± 0.1 °C and pH 7.5 (Tris-HCl buffer).

4 Conclusions

HPMC cryogels with the highest DS had the lowest wettability and swelling rate (HPMC-E), while those with the highest MS had the highest swelling rate (HPMC-J). Despite the type of HPMC used, all cryogels presented water molecules primarily in the intermediate t2 range, with only a small amount tightly bound in the t2 range of 10 ms to 100 ms. This is likely due to the presence of methyl and hydroxypropyl groups along the HPMC chains, which are not found in unsubstituted cellulose. The presence of Alkonat-L230® increased the wettability of HPMC-E cryogels possibly due to hydrophobic interaction between methyl groups and surfactant alkyl chain, with consequent orientation of polar head to the medium. A reverse orientation of the surfactant monomers was proposed in the case of HPMC-J cryogels because the swelling rate became slower.

This work demonstrated that the incorporation of CaO_2 microparticles into HPMC cryogels is a feasible strategy when slow O_2 release to the medium is required, as for instance, for biomedical applications (Willemen et al., 2021) and wastewater treatment (Amerhaider Nuar et al., 2022). However, the HPMC-E cryogels tend to be the most adequate to the incorporation of CaO_2 in order to promote a sustained release of O_2 to the medium, in agreement with the lowest wettability. The reaction of CaO_2 with water was chosen as a case study. Nevertheless, considering that the HPMC samples investigated in this study are pharmaceutical and food grades, the findings presented here are relevant for drug and food formulations, where the interaction with water might control the success of the final application.

5 CRediT authorship contribution statement

Camila Gruber Chiaregato: Investigation; methodology; data curation, writing - original draft preparation, visualization

Oigres Daniel Bernardinelli: Investigation; methodology; data curation, writing, visualization

Amin Shavandi: Conceptualization; Writing - review

Edvaldo Sabadini: Conceptualization; writing - review

Denise Freitas Siqueira Petri: Conceptualization; project administration; supervision; writing – review; funding acquisition

6 Acknowledgments

The authors thank the São Paulo Research Foundation (FAPESP) (2018/13492-2 and 2022/06284-0) and CNPq (304017/2021-3) for the financial support.

7 References

Ali, M., Farooq, U., Lyu, S., Sun, Y., Li, M., Ahmad, A., Shan, A., & Abbas, Z. (2020). Synthesis of controlled release calcium peroxide nanoparticles (CR-nCPs): Characterizations, H2O2 liberate performances and pollutant degradation efficiency. *Separation and Purification Technology*, *241*, 116729.

Amerhaider Nuar, N. N., Siti Nurul, S. N. A., Li, F., Mat Azmi, I. D., Chiang, P. C., & Choong, T. S. Y. (2022). Synthesis of Controlled-Release Calcium Peroxide Nanoparticles Coated with Dextran for Removal of Doxycycline from Aqueous System. *Polymers*, *14*(18), 1-17.

Barclay, T. G., Day, C. M., Petrovsky, N., & Garg, S. (2019). Review of polysaccharide particle-based functional drug delivery. *Carbohydrate Polymers*, *221*, 94–112.

Baumgartner, S., Lahajnar, G., Sepe, A., & Kristl, J. (2002). Investigation of the State and Dynamics of Water in Hydrogels of Cellulose Ethers by 1 H NMR Spectroscopy. *AAPS PharmSciTech*, *3*(4), 1-8.

Birk, J. P., & Walters, D. L. (1993). Pressure measurements to determine the rate law of the magnesium-hydrochloric acid reaction. *Journal of Chemical Education*, *70*(7), 587–589.

da Silva, R. L. C. G., Bernardinelli, O. D., Frachini, E. C. G., Ulrich, H., Sabadini, E., & Petri, D. F. S. (2022). Vanillin crosslinked chitosan films: The states of water and the effect of carriers on curcumin uptake. *Carbohydrate Polymers*, *292*, 119725.

de Souza, Í. F. T., & Petri, D. F. S. (2018). β-Cyclodextrin hydroxypropyl methylcellulose hydrogels for bisphenol A adsorption. *Journal of Molecular Liquids*, *266*, 640–648.

Dedhia, N., Marathe, S. J., & Singhal, R. S. (2022). Food polysaccharides: A review on emerging microbial sources, bioactivities, nanoformulations and safety considerations. *Carbohydrate Polymers, 287, 1-24.*

Dezotti, R. S., Furtado, L. M., Yee, M., Valera, T. S., Balaji, K., Ando, R. A., & Petri, D. F. S. (2021). Tuning the Mechanical and Thermal Properties of Hydroxypropyl Methylcellulose Cryogels with the Aid of Surfactants. *Gels*, *7*(3), 1-17.

Dias, S., Pedro, N., Oliveira, V., Freitas, D., & Petri, S. (2022). Hydroxypropyl methylcellulose - sugarcane bagasse adsorbents for removal of 17α - ethinylestradiol from aqueous solution and freshwater. *Environmental Science and Pollution Research*, 63936-*63952*.

Giang, H. N., Le, A. T. K., Huynh, T. N. A., Phung, T. K., & Sakai, W. (2022). Effect of additives on fabrication and properties of hydroxypropyl methylcellulose-based hydrogels. *Polymer*

Harris, G. L. (2019). Selected Laboratory and Measurement Practices and Procedures to Support Basic Mass Calibrations (2019 Ed). *National Institute of Standards and Technology*, 2–237.

Hatakeyama, T., & Hatakeyama, H. (2017). Heat capacity and nuclear magnetic relaxation times of non-freezing water restrained by polysaccharides, revisited. Journal of Biomaterials Science, Polymer Edition, *28*(10–12), 1215–1230.

Kao, C. M., Chen, S. C., Wang, J. Y., Chen, Y. L., & Lee, S. Z. (2003). Remediation of PCE-contaminated aquifer by an in situ two-layer biobarrier: laboratory batch and column studies. *Water Research*, *37*(1), 27–38.

Khalid, A., Asim-ur-Rehman, Ahmed, N., Chaudhery, I., Al-Jafary, M. A., Al-Suhaimi, E. A., Tarhini, M., Lebaz, N., & Elaissari, A. (2021). Polysaccharide Chemistry in Drug Delivery, Endocrinology, and Vaccines. *Chemistry – A European Journal*, *27*(33), 8437–8451.

Kurczewska, J. (2022). Recent Reports on Polysaccharide-Based Materials for Drug Delivery. In *Polymers, 14(19), 1-27*.

Lee, C. S., le Thanh, T., Kim, E. J., Gong, J., Chang, Y. Y., & Chang, Y. S. (2014). Fabrication of novel oxygen-releasing alginate beads as an efficient oxygen carrier for the enhancement of aerobic bioremediation of 1,4-dioxane contaminated groundwater. *Bioresource Technology*, *171*, 59–65.

Li, C. L., Martini, L. G., Ford, J. L., Roberts, M., & Ford, J. L. (2010). The use of hypromellose in oral drug delivery. *Journal of Pharmacy and Pharmacology*, *57*(5), 533–546.

Liu, C., Gao, J., Chen, X., & Zhao, Y. (2021). Effect of polysaccharides on setting and rheological behavior of gypsum-based materials. *Construction and Building Materials*, *267*, 120922.

Lodge, T. P., Maxwell, A. L., Lott, J. R., Schmidt, P. W., McAllister, J. W., Morozova, S., Bates, F. S., Li, Y., & Sammler, R. L. (2018). Gelation, Phase Separation, and Fibril Formation in Aqueous Hydroxypropylmethylcellulose Solutions. *Biomacromolecules*, *19*(3), 816–824.

Lu, S., Zhang, X., & Xue, Y. (2017). Application of calcium peroxide in water and soil treatment: A review. *Journal of Hazardous Materials*, *337*, 163–177.

Marani, P. L., Bloisi, G. D., & Petri, D. F. S. (2015). Hydroxypropylmethyl cellulose films crosslinked with citric acid for control release of nicotine. *Cellulose*, *22*(6), 3907–3918.

Martins, B. F., de Toledo, P. V. O., & Petri, D. F. S. (2017). Hydroxypropyl methylcellulose based aerogels: Synthesis, characterization and application as adsorbents for wastewater pollutants. *Carbohydrate Polymers*, *155*, 173–181.

Marzzacco, C. J. (2001). The effect of a change in the catalyst on the enthalpy of decomposition of hydrogen peroxide. *Chem 13 News*, 16–17.

Northup, A., & Cassidy, D. (2008). Calcium peroxide (CaO2) for use in modified Fenton chemistry. *Journal of Hazardous Materials*, *152*(3), 1164–1170.

Parhi, R. (2016). Development and optimization of pluronic® F127 and HPMC based thermosensitive gel for the skin delivery of metoprolol succinate. *Journal of Drug Delivery Science and Technology*, *36*, 23–33.

Pędziwiatr, P., Mikołajczyk, F., Zawadzki, D., Mikołajczyk, K., Bedka, A., Koło, S., & Oktan, N. (2018). Ric pro-akademia-cc by decomposition of hydrogen perodixe-kinetics and review of chosen catalysts. *Acta Innovations*, *26*, 45–52.

Perez-Robles, S., Carotenuto, C., & Minale, M. (2022). Effect on the Thermo-Gelation Process of the Degree and Molar Substitution of HPMC Polymer Hydrogels. *Macromolecular Symposia*, *405*(1), 2100277.

Rastinfard, A., Nazarpak, M. H., & Moztarzadeh, F. (2017). Controlled chemical synthesis of CaO2 particles coated with polyethylene glycol: characterization of crystallite size and oxygen release kinetics. *RSC Advances*, *8*(1), 91–101.

Schmidt, W., Brouwers, H. J. H., Kühne, H. C., & Meng, B. (2017). Interactions of polysaccharide stabilising agents with early cement hydration without and in the presence of superplasticizers. *Construction and Building Materials*, *139*, 584–593.

Steg, H., Buizer, A. T., Woudstra, W., Veldhuizen, A. G., Bulstra, S. K., Grijpma, D. W., & Kuijer, R. (2015). Control of oxygen release from peroxides using polymers. *Journal of Materials Science: Materials in Medicine*, *26*(7), 1–4.

Talasaz, A. H. H., Ghahremankhani, A. A., Moghadam, S. H., Malekshahi, M. R., Atyabi, F., & Dinarvand, R. (2008). In situ gel forming systems of poloxamer 407 and hydroxypropyl cellulose or hydroxypropyl methyl cellulose mixtures for controlled delivery of vancomycin. *Journal of Applied Polymer Science*, *109*(4), 2369–2374.

Thielking, H., & Schmidt, M. (2006). Cellulose Ethers. *Ullmann's Encyclopedia of Industrial Chemistry*.

Toledo, P. V. O., Bernardinelli, O. D., Sabadini, E., & Petri, D. F. S. (2020). The states of water in tryptophan grafted hydroxypropyl methylcellulose hydrogels and their effect on the adsorption of methylene blue and rhodamine B. *Carbohydrate Polymers*, *248*, 116765.

Tundisi, L. L., Mostaço, G. B., Carricondo, P. C., & Petri, D. F. S. (2021). Hydroxypropyl methylcellulose: Physicochemical properties and ocular drug delivery formulations. *European Journal of Pharmaceutical Sciences*, *159*, 105736.

Wang, H., Cui, H., Wang, X., Lin, C., Xia, S., Hayat, K., Hussain, S., Tahir, M. U., & Zhang, X. (2020). Metal complexed-enzymatic hydrolyzed chitosan improves moisture retention of fiber papers by migrating immobilized water to bound state. *Carbohydrate Polymers*, *235*, 115967.

Wang, H., Zhao, Y., Li, T., Chen, Z., Wang, Y., & Qin, C. (2016). Properties of calcium peroxide for release of hydrogen peroxide and oxygen: A kinetics study. *Chemical Engineering Journal*, *303*, 450–457.

Wei, S., Tian, B. Q., Jia, H. F., Zhang, H. Y., He, F., & Song, Z. P. (2018). Investigation on water distribution and state in tobacco leaves with stalks during curing by LF-NMR and MRI. Drying Technology, *36*(12), 1515–1522.

Wei, Y., Guo, Y., Li, R., Ma, A., & Zhang, H. (2021). Rheological characterization of polysaccharide thickeners oriented for dysphagia management: Carboxymethylated curdlan, konjac glucomannan and their mixtures compared to xanthan gum. *Food Hydrocolloids*, *110*, 106198.

Willemen, N. G. A., Hassan, S., Gurian, M., Li, J., Allijn, I. E., Shin, S. R., & Leijten, J. (2021). Oxygen-Releasing Biomaterials: Current Challenges and Future Applications. In *Trends in Biotechnology*, 39(11), 1144–1159.

Zarmpi, P., Flanagan, T., Meehan, E., Mann, J., & Fotaki, N. (2020). Biopharmaceutical Understanding of Excipient Variability on Drug Apparent Solubility Based on Drug Physicochemical Properties: Case Study—Hypromellose (HPMC). *AAPS Journal*, *22*(2), 1–15.

Zeng, A., Yuan, B., Fu, Q., Wang, C., & Zhao, G. (2009). Influence of sodium dodecyl sulfate on swelling, erosion and release behavior of HPMC matrix tablets containing a poorly water-soluble drug. *P*harmaceutical Development and Technology, *14*(5), 499–505.